A Moving-Front Transition Boiling Model

In accordance with visual observations, a transition boiling model that assumes a quench front which alternately advances and retreats in the water flow direction, is proposed. With appropriate choice of a quench zone width and heat transfer rate when the surface is wet, the model predictions are in the same range as the observed temperature oscillations. An extension of the model leads to heat transfer rate predictions in general agreement with experimental observations.

Y. K. KAO and J. WEISMAN

Department of Chemical and Nuclear Engineering
University of Cincinnati
Cincinnati, OH 45221

SCOPE

Heater wall temperature oscillations are characteristic of transition boiling. In flow boiling, the mechanism governing transition boiling depends on the volume fraction of vapor present. At high vapor volume fractions, annular flow occurs and a thin film of liquid is present on the wall during nucleate boiling. Transition boiling behavior at high volume fractions is governed by behavior in the region where this liquid film disappears.

In accordance with visual observations and temperature measurements, it was postulated that at high vapor fractions the characteristic temperature fluctuations are caused by the vertical oscillation of the edge of the liquid film on the heater surface. The temperature oscillations computed from this moving front model were compared with experimental observations taken in a test section heated by hot mercury.

The observed temperature oscillations were also used to estimate wetted area fractions during transition boiling. By relating these wetted area fractions to the aforementioned analytical model, a means for prediction of transition boiling heat transfer rates in the mercury-heated test section was developed.

CONCLUSIONS AND SIGNIFICANCE

The present work strongly supports the assumption that transition boiling temperature fluctuations in flowing systems at high vapor fractions are caused by vertical oscillations of the wetting front. Not only is this model in accord with recent visual observations, but it leads to predictions of wall temperature oscillations whose magnitudes are in general agreement with measurements. Further, it explains the high cross-correlation coefficient between temperature variations at the same axial elevation but different circumferential locations. The model also leads to heat transfer coefficient predictions which are in reasonable agreement with the experimental data. It is believed that the present model is a significant improvement over the rotating rivulet model previously used.

The oscillation of the wetting front may be expected to lead to wall temperature behavior which is highly dependent on the system under consideration. It may therefore not be possible to develop a universally applicable heat transfer correlation in terms of only the usual parameters of heat flux, wall temperature, saturation temperature, and flow quality or void fraction.

INTRODUCTION

Berenson (1962) has pointed out that in pool boiling systems, the temperature oscillations seen during transition boiling are the result of periodic wetting of the surface. Bankoff and Mehra (1962) subsequently modeled the observed wall temperature oscillations in terms of the periodic quenching of the surface.

In pool boiling, the instability of the vapor film next to the hot surface appears to induce the periodic rewetting of the hot surface. Very similar behavior is observed during flow transition boiling at low qualities or subcooled conditions. During film boiling, inverted annular flow (film of steam adjacent to heated surface) is observed. In the transition from nucleate to film boiling, the instability of the liquid-steam interface appears to induce alternate wet and dry periods. Baum et al. (1977) have proposed a model based on this instability. However, their model predicts a contact period in the range of milliseconds. At such frequencies the temperature oscillation could not be transmitted very far before it would be attenuated.

In flow boiling at high void fractions, an entirely different behavior is observed. Normal annular flow is seen with a thin film of liquid on the heated surface. The transition from nucleate to flow film boiling occurs in the narrow region where this annular film drys out. Various analytical models have been proposed for heat transfer in this region. For example, Chen et al. (1977) developed a model that considered the heat transfer from the impinging droplets and flowing steam in addition to that from liquid that periodically contacted the surface. However, they did not address the temperature oscillation phenomenon.

Argonne National Laboratory (France et al., 1979) measured the wall temperature oscillations seen at high vapor fractions during their tests of a sodium-heated steam generator. In their analysis of the Argonne data, Chu et al. (1978) adopted a model originally suggested by Hewitt et al. (1963). They proposed that the tem-

perature oscillations were due to a partial dry-out of the thin liquid film seen on the wall during annular flow. It was postulated that partial dry-out of the liquid film leads to the periodic appearance of liquid rivulets on the hot surface. The meanderings of these rivulets were assumed to cause the temperature oscillations.

The present authors simplified the rivulet model (Kao and Weisman, 1980) by assuming that the random drying and wetting of the hot surface could be approximated by a set of rivulets which moved circumferentially over the hot surface. The model allowed analytical predictions of the temperature oscillations from a mercury-heated test section as a function of the number, width, and velocity of the rivulets. In most cases, the model predicted that eight rivulets existed simultaneously over a circumference of 3.2 cm. Subsequently, T. T. Kao et al. (1982) used an essentially identical rotating rivulet model to reanalyze the Argonne temperature fluctuation data.

The flow boiling heat transfer experiments (Weisman et al., 1981) which preceded the present work, were conducted with a vertical annular test section that allowed visual observations. These tests did not support the moving rivulet model. The visual observations indicated instead that the entire wetting front moved back and forth in the vertical direction. The previously published photographs of the edge of the liquid film on the hot tube showed a somewhat irregular front but no evidence of rivulets.

The relationship of transition boiling temperature oscillations at high quality and the vertical oscillation of the wetting front is supported by the recent observations of France et al. (1982). These investigators observed the transition boiling temperature oscillations recorded by two wall thermocouples at the same axial position but at different circumferential positions. At low qualities there was little correlation between the temperature oscillations of the two couples (low cross-correlation coefficient). However, at the high qualities where annular flow is encountered, a very high degree of correlation (cross-correlation coefficients at times up to 0.96) was observed. Meandering rivulets would be expected to lead to temperature oscillations at two different circumferential locations with very low cross-correlation coefficients and hence the rivulet model cannot explain the observations at high quality. However, a quench front which alternately advances and retreats axially would be expected to produce the high cross-correlation coefficients observed. A photographic study carried out in Japan also indicates similar behavior (Nakanishi et al., 1982).

In view of the foregoing, it was decided to examine the wall temperature fluctuation data which were obtained during recent transition boiling heat transfer tests. The experimentally measured temperature oscillations at the dominant frequency were compared to predictions based on a vertically oscillating quench front.

Estimations of wetted area fractions during transition boiling have been limited. The only direct measurement known to the authors under flow boiling conditions is that of Ragheb and Cheng (1979) who used a zirconium platinum-tipped probe to measure the fraction of time during which the surface was wetted. The wall temperature fluctuations from the recent tests therefore were also used to estimate wetted area fractions and an attempt was made to relate these to the analytical model for wall temperature fluctuations.

EXPERIMENTAL PROGRAM AND RESULTS

The wall temperature fluctuations which were examined were obtained from the University of Cincinnati's heat transfer loop, which used hot mercury as the heat source. The mercury is heated outside of the test section and flows downward into the test section at a controlled temperature. Water near the saturation temperature was introduced countercurrently and was boiled by the hot mercury which was either in an outer annulus or in a central tube. The temperature-controlled heat source allowed steady-state observation of the phenomenon. Further details on the construction of the heat transfer loop are given by Weisman et al. (1981).

Temperature oscillation data were recorded in experiments with two test sections constructed of stainless steel. In the first test section, the water flowed in a round tube surrounded by hot mercury flowing in an annular space. The wall temperature was measured by thermocouples which were spot-welded onto the outer wall (mercury side) of the water tube so as not to disturb the water flow. The temperature oscillations observed were low (10°C or less) due to their attentuation by the tube wall and the mercury stream. The frequency range was between 0.2 to 0.6 Hz. There was no provision for visual observation in these tests.

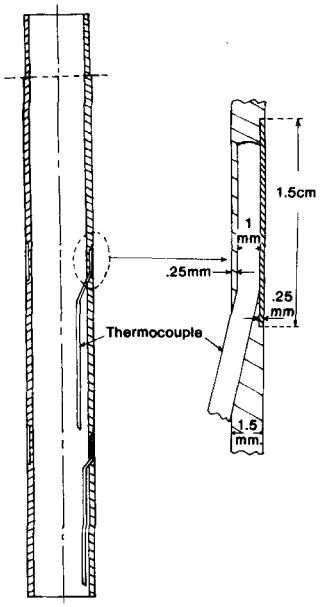

Figure 1. Installation of wall thermocouple.

A viewing window was provided in the later annular test section which was machined out of a stainless steel block. The water then flowed in an outer annulus surrounding the hot mercury flowing within an inner annular space. A total of seven sets of steady-state runs were conducted. In five of the sets, temperature oscillation data were recorded. The heat transfer data have been presented previously (Weisman et al., 1981; Wang et al., 1982).

In order to improve the wall temperature measurement, stainless steel sheathed, 1 mm OD, MgO insulated thermocouples were embedded within the stainless steel wall between the water and mercury, as shown in Figure 1. It was concluded that the effective depth of the junctions was somewhere between 0.25 mm (thickness of stainless steel sheath) and 0.76-mm (location of thermocouple wires) from the surface.

Because of the close proximity of these thermocouples to the water-wall interface, the temperature oscillations observed were now much larger (30°C) than those previously seen with the round tube test section. The magnitude and frequency of the temperature oscillations were very similar to those previously seen in the Argonne National Lab steam generator tests (France et al., 1979, 1982).

Figure 2 shows three typical temperature response curves from a couple which was in the transition region. The variation in the three curves reflects the distance between the center of the quench front oscillation and the thermocouple position. Because the thermocouple was read as a differential couple opposed to a couple in the mercury stream at a higher temperature, a high voltage indicates a lower wall temperature. Thus, in the curve at the left which was below the center of oscillation, the thermocouple position is wet most of the time. The temperature oscillations in the left hand figure, show that the surface is generally at a low temperature. The central curve reflects a couple in the center of the front oscillation. The temperature oscillations are large and indicate nearly equal wet and dry periods. In the

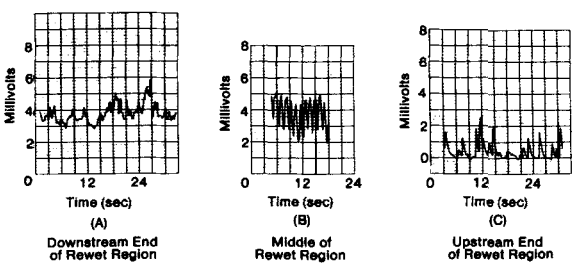

Figure 2. Typical temperature oscillations.

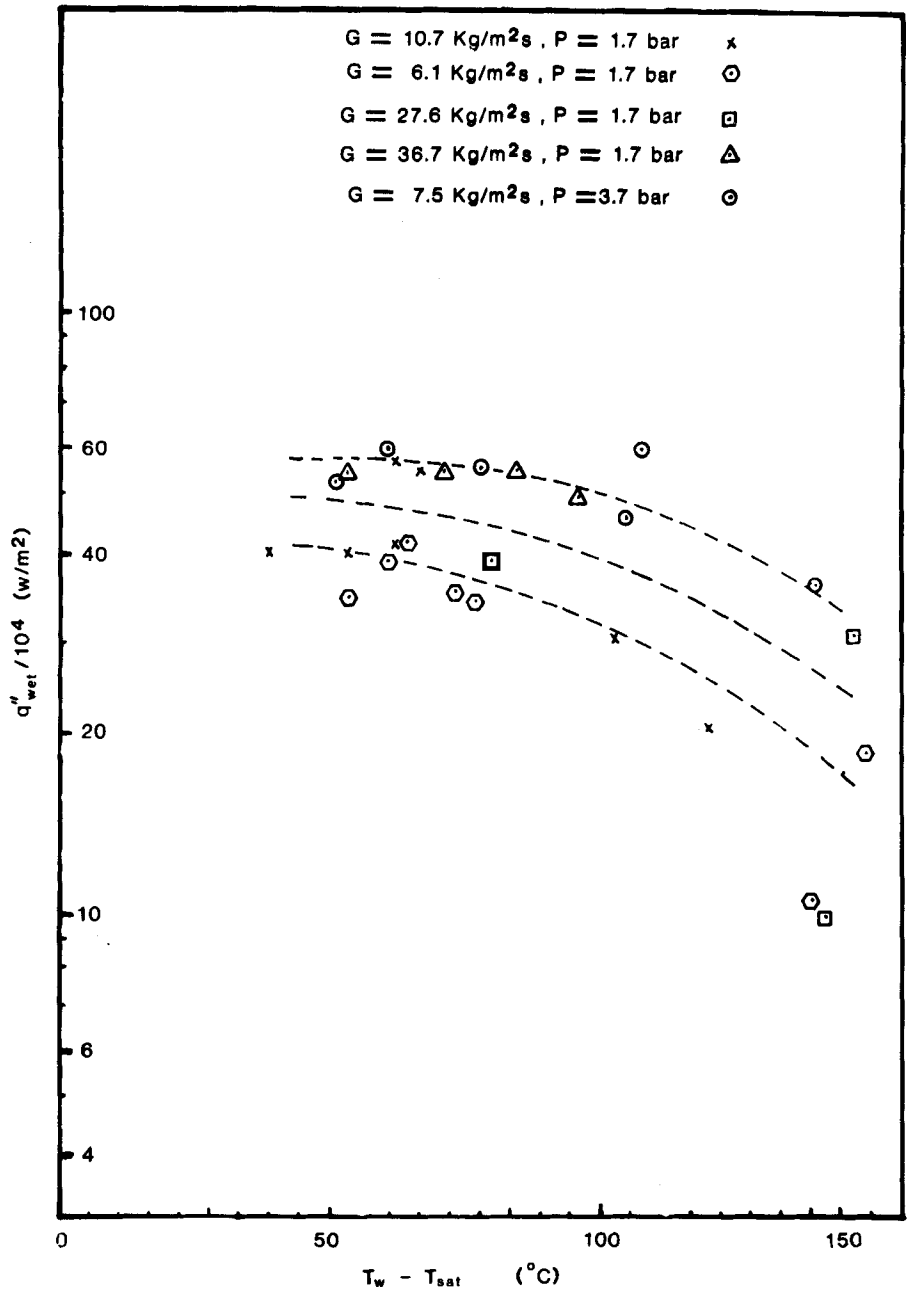

Figure 3. Relationship between wetted heat flux and ΔT_{sat}.

right hand curve, the thermocouple is above the center of the front oscillation where the surface is generally dry. The temperature curves clearly show that low surface temperatures are sustained for only brief periods.

Estimation of Wetted Area Fraction

As may be seen from Figure 2, the thermocouple response to a change in conditions at the water-wall interface was rapid. Under most circumstances, the time when the surface is wetted can now be determined from the change in the direction of temperature response. By assuming that the surface is wet during the period when the temperature is generally dropping or at a low value, and dry when generally rising or at a high value, the fraction of time when surface is wet can generally be obtained from these temperature response curves.

By making the assumption that when the surface is dry the heat transfer rate corresponds to the low rate seen at the end of the transition region, we may use the overall heat transfer data and wetted fraction to compute the heat transfer rate while the surface is wetted, q''_{wet}. The results of these calculations are shown in Figure 3. It may be seen that the heat transfer rate during the period when the hot surface is wetted does not increase sharply, as was in the case of nucleate pool boiling, with rising surface temperature. Instead, the rate stays at approximately at the CHF value and decreases slightly as the surface temperature increases. The wetted heat transfer rate is higher at the higher mass fluxes. This behavior is in general agreement with the observations of Rahgeb and Cheng (1979) and the conclusion of Kao and Weisman (1980). The failure of the heat flux to increase as surface temperature increases cannot be explained by Chen's suppression effect (1966), because according to Chen's correlation the experimental flow rates are too low for any significant boiling suppression to be seen. The alternative suppression factor recently proposed by Bjorge et al. (1982) would also fail to provide an explanation.

Analysis of Temperature Oscillations

As may be seen in Figure 2, the actual temperature oscillations are highly complex. In view of this, a Fourier analysis of the oscillations was conducted. Figure 4 shows two typical frequency spectra obtained. In most cases the peak was observed in the range of 0.4–0.6 Hz. A secondary peak (in some cases this was the major peak) was observed at very low frequencies of the order of 0.2–0.1 Hz. Additional smaller peaks in the high frequency range (above 0.7 Hz) were also seen.

The frequency spectrum can be related to the visual observation of the wetting front. Clear visual observations are possible when the water flow on the viewing window is not too turbulent. The wetted surface can then

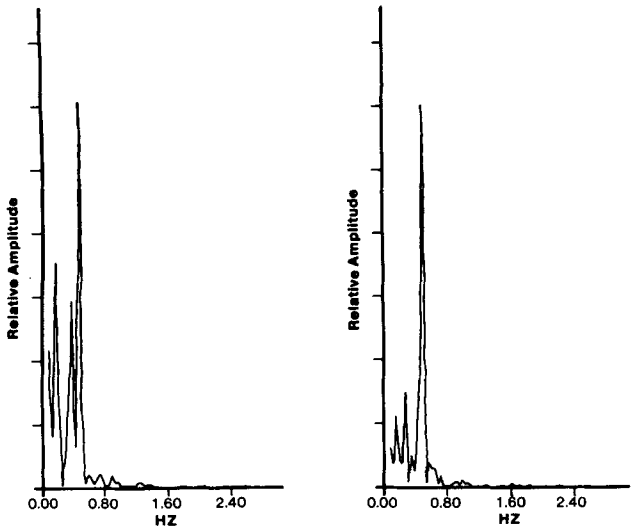

Figure 4. Typical frequency spectra.

be readily identified by a dark region on the hot surface. Such observations are possible at low and moderate mercury inlet temperatures. The axial oscillation of the quenching front cannot be seen readily at higher mercury temperatures as the high steam flow rate causes the water next to the viewing window to become very turbulent. It then becomes impossible to see the hot surface underneath. However, the temperature responses were similar to the cases when front movement was discernible, and therefore it is reasonable to assume that the same behavior prevailed underneath the hot surface. Photographs of the quench front are provided by Weisman et al. (1981) and Wang et al. (1982). Although the motion of the quench front is somewhat chaotic, indicating the stochastic nature of transition boiling, it is possible to distinguish four general types of motion:

1. A more or less regular axial oscillation of the entire wetting front with a frequency of about 0.5 Hz.
2. A slow, less regular, up-and-down wandering of the center of the quench front oscillation.
3. A higher-frequency (above 0.5 Hz) oscillation of the liquid at the quench front interface giving an irregular and constantly changing interface.
4. Occasional dry patches appearing for short times in the region below the nominal quench front.

The more or less regular axial oscillation of the quench front would appear to account for the peak in the 0.4–0.6 Hz range. The slow wandering of the center of the quench front accounts for the low frequency peak. The higher frequency content is explained by the irregular and changing quench front interface plus the occasional dry patch appearance.

Since the more or less regular axial oscillation of the quench front appeared to dominate the behavior, Fourier analysis was used to segregate this behavior. The coefficients obtained from the Fourier analysis for frequencies between about 0.3 and 0.8 Hz were therefore used to reconstruct the temperature oscillations due to the simple axial oscillation of the wetting front. The average frequency and magnitude (max. temp. − min. temp.) of the reconstructed temperature oscillations obtained in a typical run is shown in Figure 5. The error bars on the magnitude indicate twice the standard deviation of the reconstructed oscillation magnitudes over the time period for which the Fourier analysis was conducted. The frequency error bar shows the range of the oscillation components included in the analysis. The error bars for the surface temperature, reflecting twice the standard deviation of the surface temperature, have been discussed previously (Weisman et al., 1981).

Those points in Figure 5 which are not identified by squares were obtained by simple visual analysis of the temperature oscillation data. The frequencies were obtained by counting the number of cycles per unit time and the magnitudes by measuring the average height of the oscillation. It was necessary to proceed in this manner for all those points where the temperature oscillation magnitudes were too low to allow for effective digitalization of the data. It is recognized that this is not entirely consistent with the Fourier analysis procedure but these points were not used for comparison with the proposed model.

Examination of Figure 5 shows that the reconstructed oscillation magnitudes have their highest values at average wall temperatures roughly midway between the temperatures seen when the surface is all wet and when it is all dry. The magnitudes decrease toward both ends of the wall temperature range. The reconstructed frequency of the large temperature oscillations remains fairly constant over the range of interest.

MOVING QUENCH FRONT MODEL

It is proposed that the axial oscillation of the quench front in the flow direction is the major cause of the temperature oscillations that characterize transition boiling at high void fractions. The heat transfer rate is very high when the hot surface is covered with water. When the liquid film recedes from an area, there is a drastic drop in the heat transfer rate. This change in the heat transfer rate leads to the observed temperature variation.

To predict the temperature oscillations, the test section energy balance was analyzed. The analysis included both the flowing mercury and the stainless steel wall between the hot mercury and the water stream. At a mercury flow rate of 0.14 m/s (1,615 ft/hr), the hydrodynamic boundary layer is much thinner than the thermal boundary layer. The mercury may therefore be considered to be in rodlike flow. Previous studies (Weismann et al., 1981; Wang et al., 1982) of the heat transfer in this test section have shown that:

a) Axial conduction in the mercury accounts for a negligible fraction of the axial heat flow, and

b) The effective radial thermal diffusivity in the mercury stream was several times the molecular diffusivity.

The mercury energy balance then becomes

$$\frac{\partial T_m}{\partial t} + u_z \frac{\partial T_m}{\partial z} = \alpha_{\text{eff}} \frac{1}{r} \frac{\partial}{\partial r}\left(r \frac{\partial T_m}{\partial r}\right) \tag{1}$$

where

α_{eff} = effective thermal diffusivity assigned to mercury (provides match between calculated and observed central mercury temperatures).

The energy balance for the stainless steel wall is

$$\frac{\partial T_s}{\partial t} = \alpha_s \left[\frac{1}{r} \frac{\partial}{\partial r}\left(r \frac{\partial T_r}{\partial r}\right) + \frac{\partial^2 T_r}{\partial z^2}\right] \tag{2}$$

The previous studies showed that there was a contact resistance. ($h_c \simeq 18{,}000$ W/m^2°C). Therefore

$$T_s = T_m - \frac{q''}{h_c} \qquad \text{at } r = r_1 \tag{3}$$

A sealed center tube of OD r_o is located in the mercury stream. Three thermocouples are spot-welded inside the sealed tube to monitor the temperature there. Because there is no heat transfer at the central tube,

$$\frac{\partial T_m}{\partial r} = 0 \qquad \text{at } r = r_o \tag{4}$$

At the outer water and wall interface and any axial location it is assumed that

$$-k_s \frac{\partial T_s}{\partial r} = q''_{\text{wet}} \tag{5}$$

when the surface is in contact with water; and

$$-k_s \frac{\partial T_s}{\partial r} = q''_{\text{dry}} \qquad \text{at } r = r_2 \tag{6}$$

when the surface is dry.

The hot mercury line to the test section was insulated so that at the upper end of the test section the mercury and the wall are at a uniform temperature, $T_{m,\text{in}}$

$$T_s = T_m = T_{m,\text{in}} \qquad \text{at } z = 0 \text{ for all } r \tag{7}$$

There is no significant heat transfer at the bottom end of the test section in the axial direction in the steel wall, so it is assumed that

$$\frac{\partial T_s}{\partial z} = 0 \qquad \text{at } z = L \text{ for all } r \tag{8}$$

Within the transition boiling region, the boundary conditions at the water-wall interface change from wet to dry in accordance with the back and forth motion of the quench front. The order of

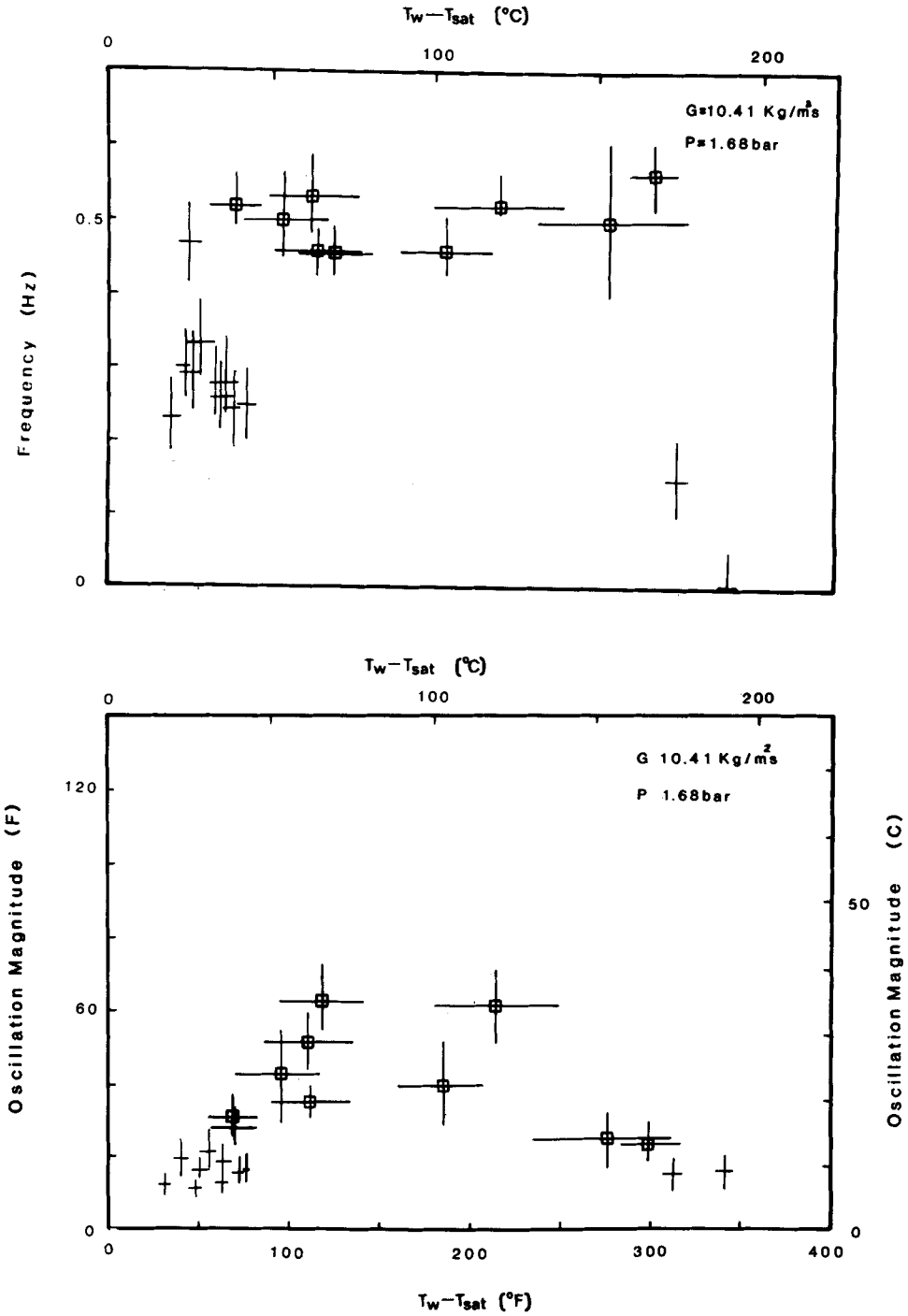

Figure 5. Frequency and magnitude of temperature oscillation in Run 600; flow rate = 27.58 kg/m²·s, pressure = 1.68 bar (168 kPa).

magnitude change in wall heat flux produced by this motion leads to a rather difficult numerical problem which is further complicated by the specification of a heat flux boundary condition.

Numerical Procedure

If the system is discretized and a standard finite difference method is used to solve the resulting model equations, a large number of grid points are needed in the quench front region to obtain a satisfactory truncation error. This leads to severe restrictions on the largest time step which can be used if an explicit method is used for integration in the time domain. While an implicit method could be used to eliminate this time step restriction, the flux-type boundary condition would seem to require that a trial and error procedure be used to meet the boundary conditions at the water-wall interface.

To avoid the foregoing problems, the orthogonal collocation procedure was used instead to obtain a numerical solution. The sharp change in heat flux conditions suggested that the solution for the entire test section be obtained by dividing the test section into several segments and appropriately matching the segment solutions at the segment boundaries. This is the so-called spline collocation method (Villadsen and Michelsen, 1978).

Since the length of the quench front region is not known a priori and has to be determined by matching the model with experimental data, it is convenient to break this test section into four segments. Two middle segments are reserved for the quench front region centering around its average location. One of the remaining segments is placed above the quench front region, where the surface is always dry. The other segment is placed below the quench front region, where the surface is always wet. The length of an individual segment can be adjusted independently in accordance

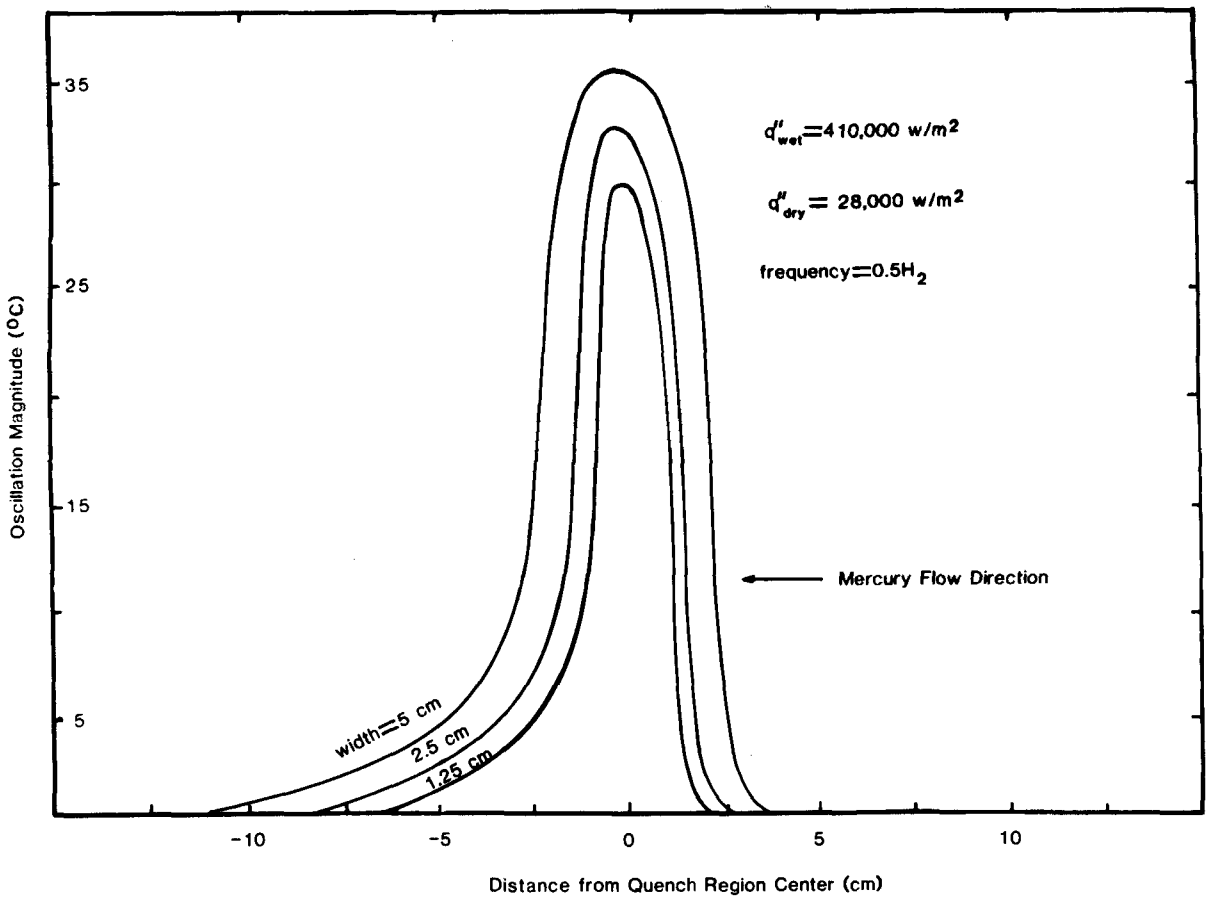

Figure 6. Calculated magnitude of temperature oscillations at $q''_{wet} = 4.1 \times 10^5 W/m^2$, $q''_{dry} = 2.6 \times 10^4 W/m^2$, frequency of oscillation = 0.5 Hz.

with the size and the location of the quench front region.

To facilitate the programming so that the model parameters (such as length of the wetting front, its location, and the inlet mercury temperature) could be easily adjusted, the model equations, Eqs. 1–8, were recast into dimensionless form.

The temperature oscillation is predominantly affected by the wet boundary condition. In terms of the dimensionless temperature, τ, defined by

$$\tau = (T - T_{sat})/(T_{m,in} - T_{sat}); \tag{9}$$

Eq. 5 becomes

$$-\frac{\partial \tau_s}{\partial y_s} = \frac{q''_{wet}\Delta r_s}{k_s(T_{m,in} - T_{sat})} \tag{10}$$

where y_s = the normalized wall radial coordinate = $r/\Delta r_s$ and Δr_s = wall thickness. This suggests that temperature oscillations can be standardized with the factor $q''_{wet}/(T_{m,m} - T_{sat})$. This approach was taken in comparing the model predictions with the experimental data.

A computer program embodying the foregoing model was devised and used to predict wall temperature oscillations as a function of model parameters.

Model Characteristics

Figure 6 shows the magnitude of temperature oscillations (max temp–min temp) predicted by the model at the thermocouple location when the wetted heat flux is $4.10 \times 10^5 W/m^2$ (1.3×10^5 Btu/h·ft²) and the dry flux is $2.84 \times 10^4 W/m^2$ (9×10^3 Btu/h·ft²) for three different quench front region widths (length over which quench front oscillates) at an oscillation frequency of 0.5 Hz. The magnitudes are plotted against distance from the centerline of the quench front oscillation. Note that the oscillation magnitudes decrease sharply over narrow regions at both ends of the quench front region. This provides an explanation of the paucity of experimental data in the intermediate oscillation magnitude range since it is much less likely that the thermocouples in test section will sense oscillations in that range.

It is interesting to observe that the maximum value of the temperature oscillations is not substantially affected by the choice of the front width. The magnitude is only slightly higher for longer widths. Visual observation indicated that the front width was of the order of 2.5 cm although longer widths were sometimes seen. Since the magnitude of maximum temperature oscillations was not substantially influenced by front width, and to be consistent with the visual observations, a quench front width of 2.5 cm is used in subsequent comparisons.

It may also be seen from Figure 6 that observable temperature oscillations occur outside of the quench zone. These are seen mostly downstream from the quench region. These temperature oscillations are caused primarily by temperature oscillations in the mercury being transmitted downstream by the flowing fluid and to a much lesser extent by the axial conduction in the steel wall. In the present apparatus, temperature oscillations are therefore not necessarily indicative of transition boiling.

Figure 7 shows time variation in wall temperature at four different axial locations at different wetted area fractions at the depth corresponding to the thermocouple location (assumed as 0.25 mm). Wet and dry heat fluxes and oscillation frequency are fixed at the values used for Figure 6. The oscillations are largest when the wetted fraction is about 0.5. Temperature oscillations are smaller when the surface is either dry or wet most of the time. The latter cases exhibit an interesting phenomenon in that the temperature response changes its direction gradually when the surface changes from mostly dry to mostly wet. Furthermore, the change begins slightly before the front reaches the axial location being observed.

Figure 8 shows temperature oscillations computed at three increasing distances from the water-wall interface at a fixed axial location (fixed wetted fraction). The temperature oscillation

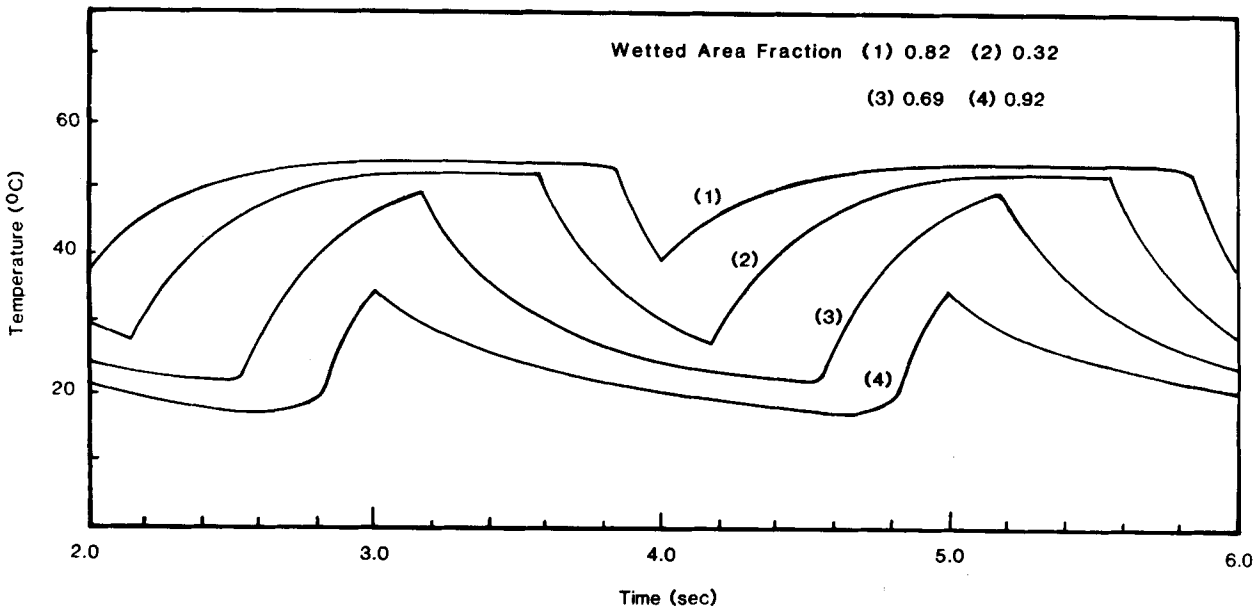

Figure 7. Calculated temperature responses at four different wetted area fractions at the thermocouple location ~10 mil (2.5 cm) from the surface; front width is 1 in. (2.5 cm).

magnitude decreased as the distance from the water-wall interface increases. The location farthest from the water-wall interface corresponds roughly to the thermocouple location in the round tube test section. In that test section the thermocouples were located next to the wall in the mercury stream. The predicted oscillation magnitudes at this location are also in reasonable agreement with maximum oscillation magnitudes observed in the round tube test section, (Kao and Weisman, 1980).

COMPARISON OF MODEL WITH EXPERIMENTAL DATA

The most important model parameters are the width of the moving quench front region, the wetted heat transfer coefficient and the frequency of oscillation. As indicated previously, the width of the quench front was taken as about 2.5 cm. The last two parameters were estimated from experimental data to be in the ranges of 3.45×10^5 to 5.7×10^5 W/m^2 (110,000 to 180,000 Btu/hr·ft^2) (Figure 3) and around 0.5 Hz (Figure 5), respectively. Although the data indicated that the wetted heat flux decreased somewhat with increasing temperature, the present model was restricted to a wetted heat flux which was invariant with surface temperature.

At each inlet water flow rate examined, transition boiling data were obtained over a range of inlet mercury temperatures, $T_{m,\text{in}}$. As indicated by Eq. 10, the analytical predictions of the behavior at these diverse conditions could be brought together by multiplying the oscillation magnitudes and $(\overline{T}_{m,\text{in}} - \overline{T}_w)$ by the quantity

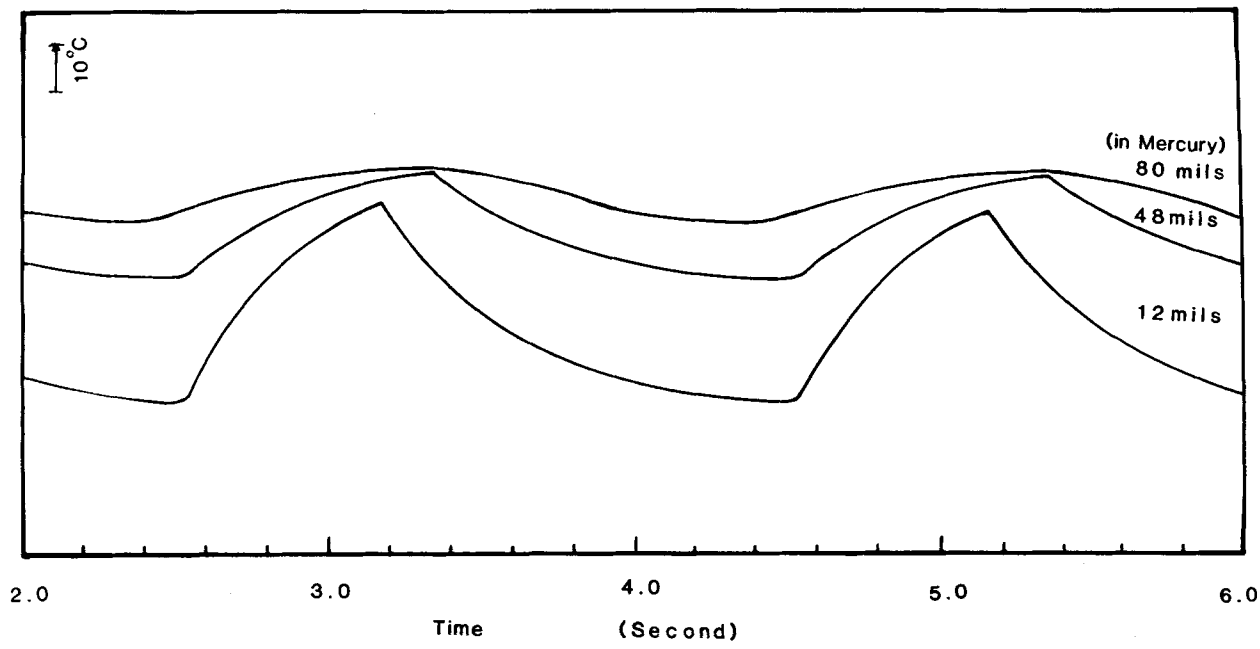

Figure 8. Calculated temperature at three different depths from the surface

$$\left\{\begin{array}{l} q''_{\text{wet}} = 4.1 \times 10^5 \text{W/m}^2\text{, front width} = 1 \text{ in. (2.5 cm)} \\ q''_{\text{dry}} = 2.6 \times 10^4 \text{W/m}^2\text{, wetted fraction} = 0.685 \end{array}\right\}$$

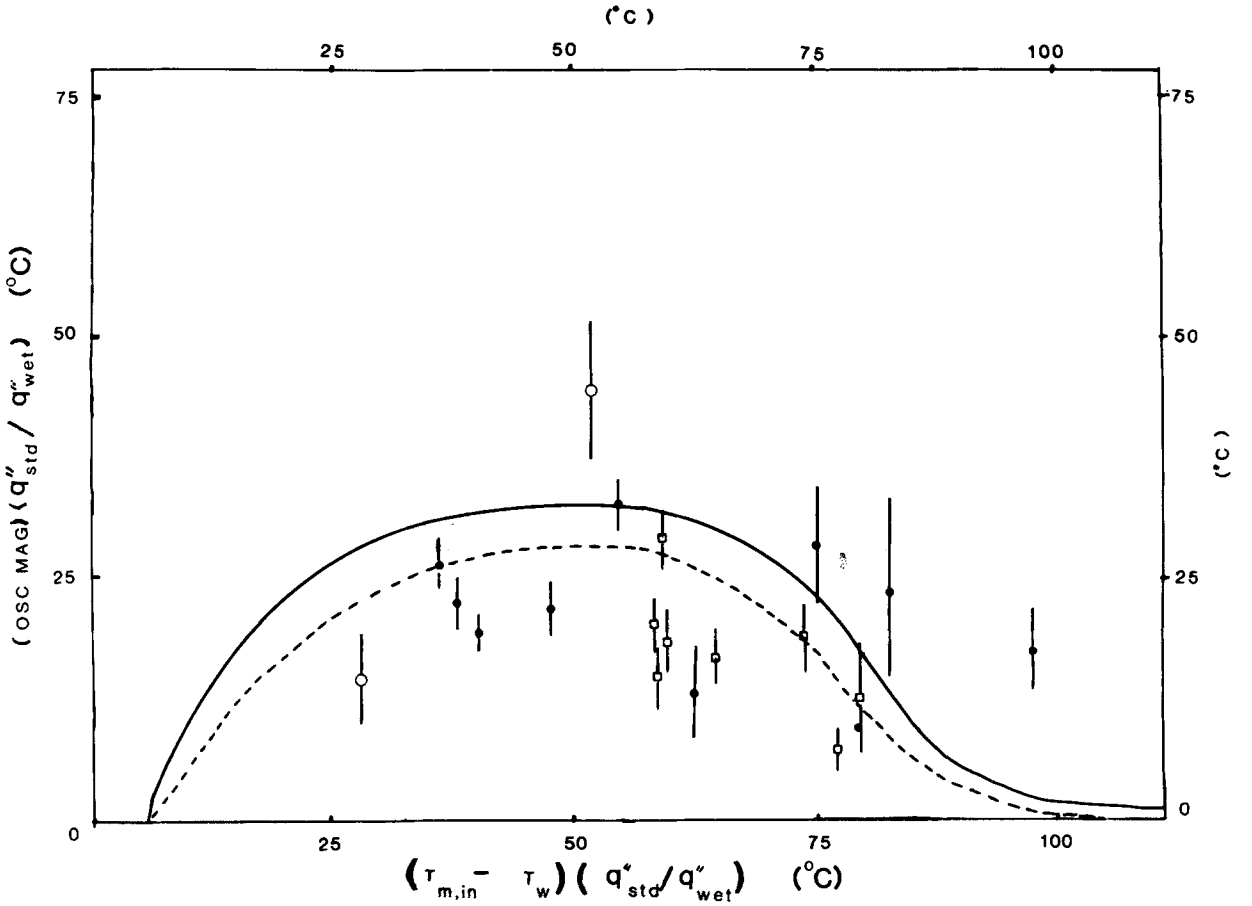

Figure 9. Comparison of observed and computed temperature oscillations.

(q''_{std}/q''_{wet}) where q''_{wet} designates the heat flux while the wall is wetted. The value of q''_{std} was set at 4.1×10^5 W/m^2 (130,000 Btu/hr·ft^2). Figure 9 compares the reduced experimental data points and the model predictions. The reduced oscillation magnitudes are shown as a function of $(\overline{T}_{m,in} - \overline{T}_w) \times (q''_{std}/q''_{wet})$ for thermocouples at depths of 0.025 and 0.076 cm (10 mils and 30 mils). (It will be recalled that the effective thermocouple depth is believed to be in this range). Only those data points derived from oscillations with appreciable magnitudes (such as those indicated by squares in Figure 5) are shown.

The theoretical predictions of the oscillation magnitude are in the correct range but there is considerable scatter. Over much of the range the magnitude of the observed oscillations tends to be below the predicted curve. This may be attributed to the fact that the predictions were based on the assumption that the heat transfer rate where the wall was wetted remained constant at the critical heat flux. Actually, the heat fluxes decrease as the wall temperature increases (Figure 3). We would therefore expect that the magnitude of the actual temperature oscillations would be below those calculated, particularly at high wall temperatures [low values of $(\overline{T}_{m,in} - \overline{T}_{wet})$]. A curve based on a heat flux decreasing with temperature would probably provide a somewhat better fit of the observed data.

The analytical approach leads to a single curve of the wetted fraction, f, vs. $(\overline{T}_{m,in} - \overline{T}_w)(q''_{std}/q''_{wet})$. The computed curve is compared to the experimentally derived wetted fraction in Figure 10. The experimental data show relatively little scatter when treated in this fashion, but high wetted fractions are reached at lower wall temperatures (greater values of $(T_{m,in} - T_w)$ than predicted. This is consistent with the fact that significant temperature oscillations (Figure 9) persist at wall temperatures lower than those that are predicted for the termination of large temperature oscillation. A possible explanation for this behavior may lie in the fact that the edge of the quench front is actually highly irregular rather than the simple plane edge assumed by the model. While the simple edge assumed in the model may represent the average location of the front, the wall would really not be fully wetted at the end of assumed oscillation distance but at a somewhat lower elevation and hence lower temperature. An additional factor may be, as seen in Figure 7, that at high wetted fractions the wall temperature begins to increase before the dry front arrives. This could have led to a slight underestimate of the wetted area.

It appears that the simplified vertically oscillating quench front model can explain the general features of the observed temperature oscillations. Although there are discrepancies between the quantitative prediction of the model and experimental observations, the discrepancies are of a nature which can be accounted for by the simplifications made.

Heat Transfer Predictions

The fact that the model leads to the single curves of Figures 9 and 10 for all of the data suggests that the analytical model could lead to heat transfer predictions. To reduce the relationship between the predictions and the specific apparatus used to obtain the present data, it was desired to eliminate the reliance on the inlet mercury temperature, $\overline{T}_{m,in}$. For a given value of $\overline{T}_{m,in}$, the analytically derived curves show that the range of wall temperatures over which significant wall temperature oscillations occur is fixed. The all-wet or all-dry conditions are associated with particular values of $(\overline{T}_{m,in} - \overline{T}_w)(q''_{std}/q''_{wet})$.

Now consider the difference in temperature between the conditions at which the wall is fully wetted and the average temperature at which the wetted fraction is f_t. For the average wall temperature corresponding to f_t, designated as $\overline{T}_{w,t}$, the value of $(\overline{T}_{m,in} - \overline{T}_{w,t})(q''_{std}/q''_{wet})$ is fixed. Similarly, for the all wet condition, $(\overline{T}_{m,in} - \overline{T}_{w,wet})(q''_{std}/q''_{wet})$ is fixed. For any given value of $T_{m,in}$ the difference between these quantities is

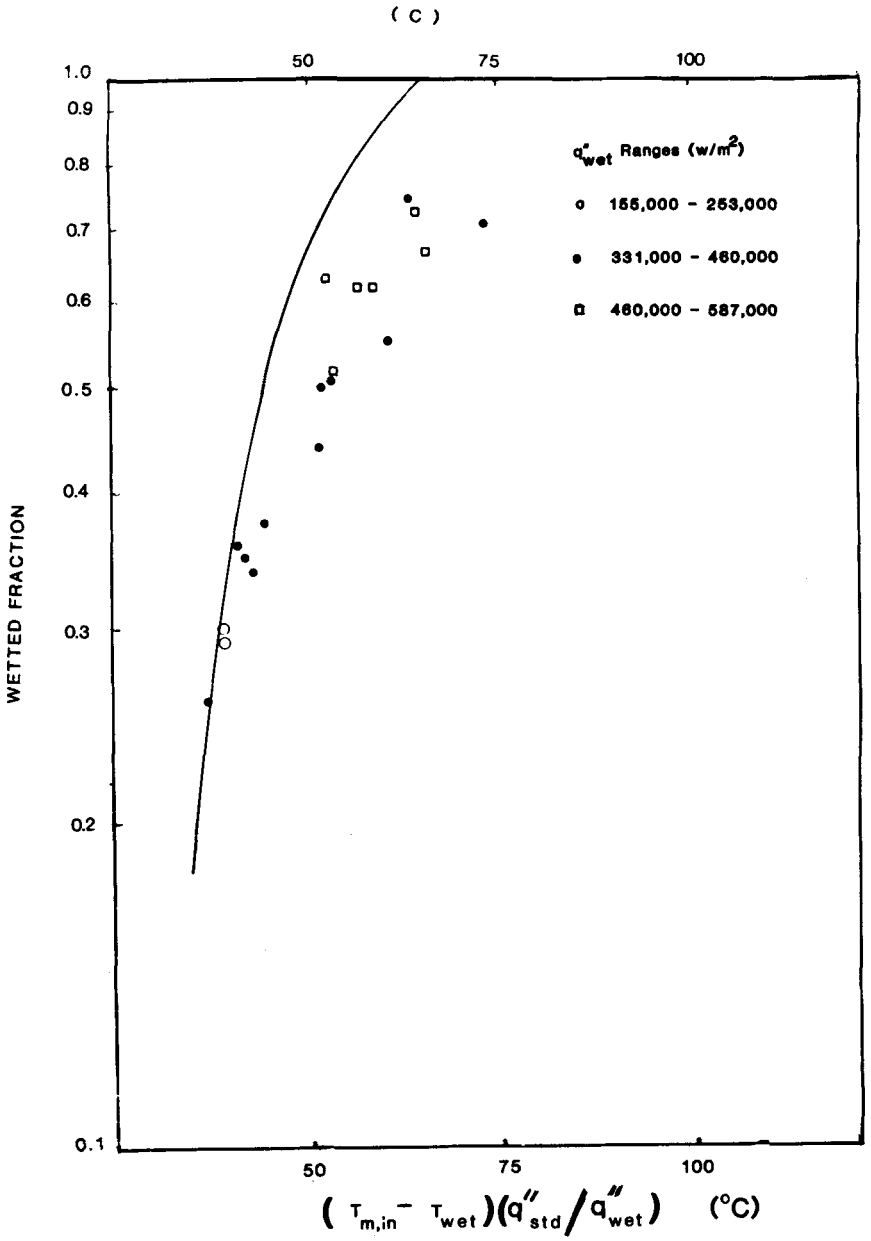

Figure 10. Observed and computed wetted fractions.

$$(\overline{T}_{m,\text{in}} - \overline{T}_{w,\text{wet}})(q''_{\text{std}}/q''_{\text{wet}}) - (\overline{T}_{m,\text{in}} - \overline{T}_{w,i})(q''_{\text{std}}/q''_{\text{wet}}) = (\overline{T}_{w,i} - \overline{T}_{w,\text{wet}})(q''_{\text{std}}/q''_{\text{wet}}) \quad (11)$$

or

$$\Delta T_{\text{eff}} = (\overline{T}_{w,i} - \overline{T}_{w,\text{wet}})(q''_{\text{std}}/q''_{\text{wet}}) \quad (12)$$

Since the same expression would be obtained for any given value of $\overline{T}_{m,\text{in}}$, a given value of f is associated with a given value of ΔT_{eff}. When $\overline{T}_{w,i}$ equals $\overline{T}_{w,\text{wet}}$, ΔT_{eff} is zero and f is zero.

To calculate $\overline{T}_{w,\text{wet}}$, it is assumed that the standard nucleate boiling heat transfer correlations apply. We therefore use the McAdams (1949) correlation for water boiling at near atmosphere pressure; that is

$$q''_{\text{wet}} = 2.25\,(\overline{T}_{w,\text{wet}} - T_{\text{sat}})^{3.86} \quad (13)$$

where q'' is in W/m^2 and T is in °C. The foregoing approach is used in Figure 11 where the wetted fraction is plotted against ΔT_{eff}. It may be seen that the data are well correlated by this procedure.

If the analytical model which has been proposed has a reasonable validity, then we would expect that the total heat flux, q''_t, should be given by

$$q''_t = fq''_{\text{wet}} + (1-f)q''_{\text{conv}} = fq''_{\text{wet}} + (1-f)h_c\,(\overline{T}_w - \overline{T}_{\text{sat}}) \quad (14)$$

and

$$h_t = q''_t/(\overline{T}_w - \overline{T}_{\text{sat}}) \quad (15)$$

To use this approach for prediction of heat transfer coefficients, a means for prediction of q''_{wet} is required. If we assume, as we did in developing the model for prediction of wall temperature oscillation, that q''_{wet} is equal to the critical heat flux, then q''_{wet} may be predicted following the approach previously used for predicting the critical heat flux. Wang et al. (1982) have recommended that at the low flows of the present test, q''_{crit} be obtained from the curve of Griffith et al. (1978). These latter investigators concluded that at low flows, the ratio of q''_{wet} to q''_{crit} at pool boiling conditions is directly related to the local void fraction.

The forced convection heat transfer coefficient for steam was also estimated following the suggestion of Wang et al. (1982). They predicted h_c by means of the Quinn's (1963) correlation. For annuli, Quinn suggested

$$h_c = .023(k_B/D)(\mu_B/\mu_w)^{0.14}Pr_B\left(\frac{GDx}{\mu_B}\right)^{0.8}\left[1 + \frac{(1-x)}{x}\frac{\rho_B}{\rho_\ell}\right]^{0.8} \quad (16)$$

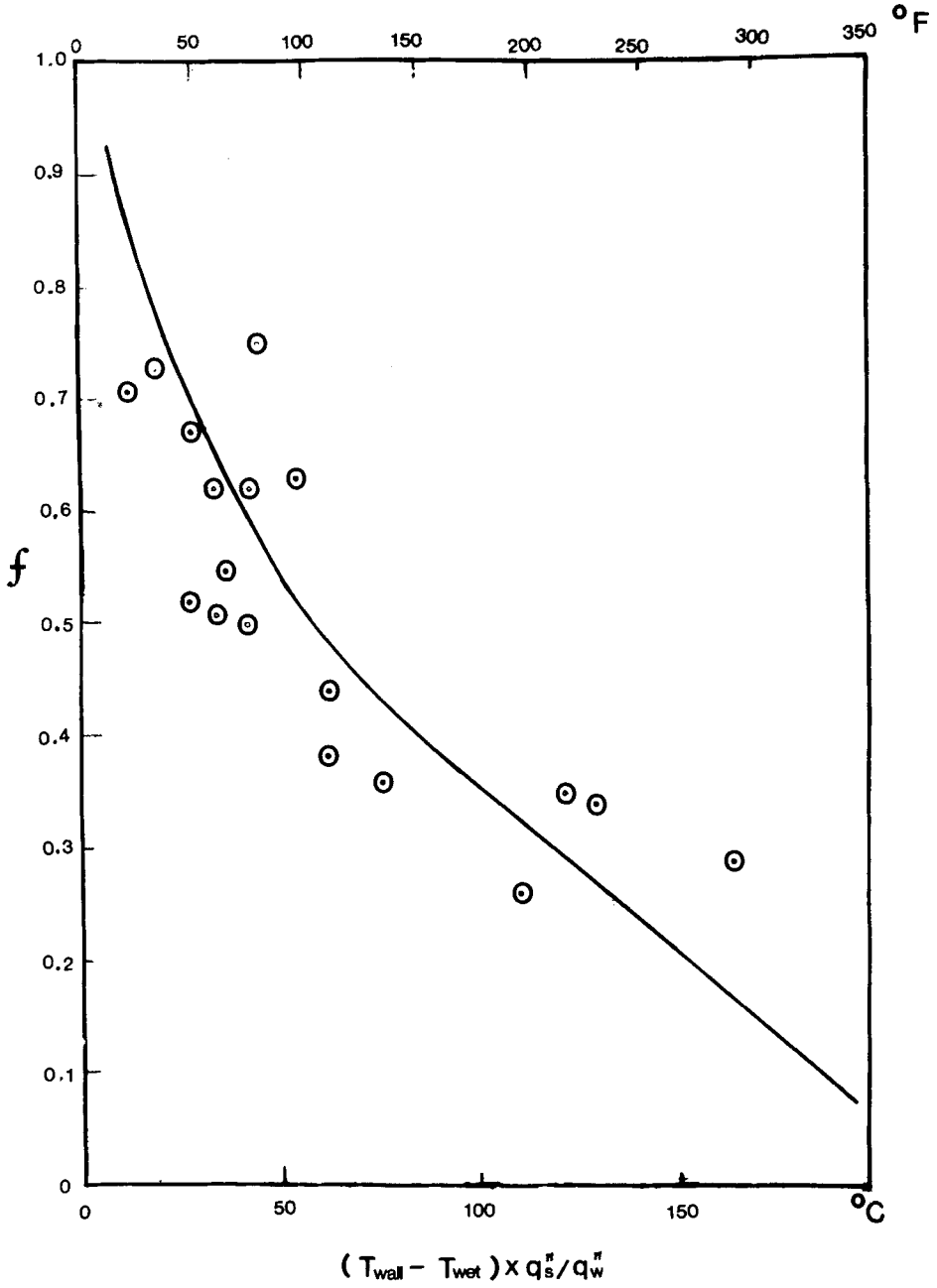

Figure 11. Wetted fraction correlation.

This correlation tends to underestimate h_c since the effect of heat transfer to droplets striking the wall is neglected. However, the total convective heat transfer coefficient is small and its value does not substantially affect the result.

Figure 12 shows a parity plot in which the measured heat transfer coefficients for the uppermost thermocouple are compared to the predictions via Eq. 14. The value of q''_{wet} was taken as q''_{crit} obtained from Griffith et al. (1978) and h_c was obtained from Eq. 16. Values of f were computed from Figure 10. It may be seen that the comparison is quite reasonable although there is substantial scatter.

It is useful to compare the predictions shown in Figure 12 with the predictions obtained from the entirely empirical correlation reported by Wang et al. (1982). Based on work by Pei (1980), they also fitted their data by taking the transition boiling heat transfer coefficient as equal to the sum of a convective component, h_c, and a boiling component, h_b. The small convective component was obtained from Quinn's correlation (Eq. 16) and the boiling component from

$$h_b = h_m e^{-0.05\Delta T} + 4{,}500\left(\frac{G}{G_{ref}}\right)^{0.2} e^{-0.012\Delta T} \tag{17}$$

where

$$\Delta T = (\overline{T}_w - T_{sat}) - \Delta T_{crit}$$

$$\Delta T_{crit} = (q''_{crit}/2.253)^{1/3.86}$$

$$G_{ref} = 68 \text{ kg/m}^2\text{-s}$$

For $G \le G_{ref}$

q''_{crit} = critical heat flux from Griffith et al. (1978) = $q''_{crit\,A}$

For $G > G_{ref}$

$$q''_{crit} = q''_{crit\,A}(G/G_{ref})^{0.33}$$

The value of q''_t is then obtained from

$$q''_t = (h_b + h_c)(\overline{T}_w - T_{sat}) \tag{18}$$

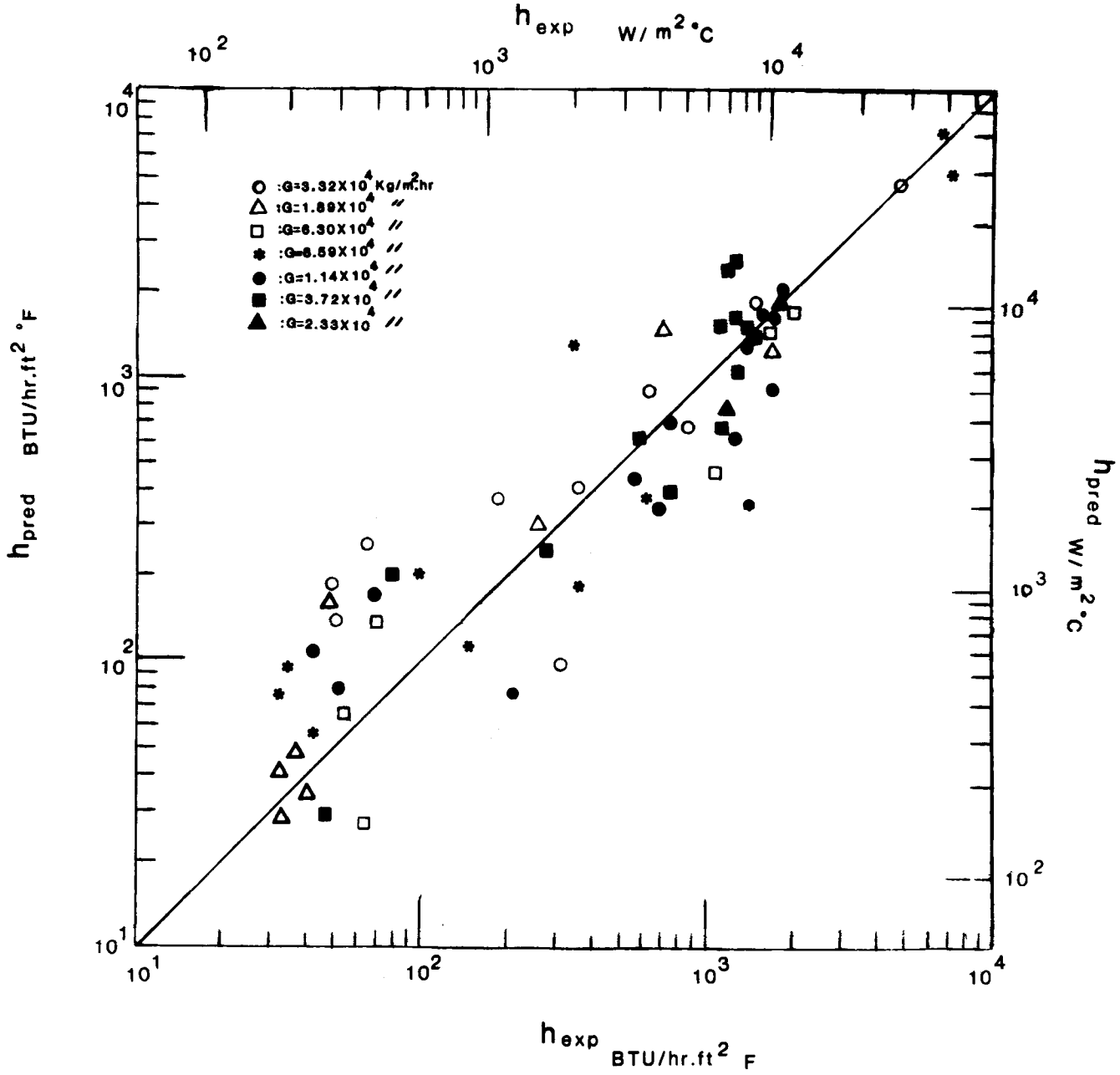

Figure 12. Comparison of predicted and observed heat transfer coefficients.

To compare the two transition boiling heat transfer correlations, the ratio, R is defined as

$$R = \frac{\text{Predicted heat transfer coefficient}}{\text{Measured heat transfer coefficient}} \tag{19}$$

A statistical comparison of the points shown in Figure 12, based on the use of the ratio R, is shown in Table 1.

It may be seen that both of the correlations tend to overpredict the data somewhat and both show very substantial scatter [high $\sigma(R)$]. However, the value of $\sigma(R)$ for the present approach is only about 25% greater than that of the strictly empirical correlation.

TABLE 1. COMPARISON OF TRANSITION BOILING HEAT TRANSFER CORRELATIONS

Correlation	$\mu(R)$	$\sigma(R)$
Present (q''_{wet} constant)	1.18	0.77
Revised (q''_{wet} decreases with T_w)	1.03	0.60
Previous Empirical	1.11	0.63

It was believed that both the overprediction of the present correlation and the value of $\sigma(R)$ could be reduced by a more realistic treatment of the heat flux during the wetted period. It will be recalled (see Figure 3) that the heat flux did not remain constant but declined somewhat with increasing wall temperature. If we approximate the heat flux variation by

$$q''_{wet} = q''_{crit} \exp[-1.6 \times 10^{-3} (\overline{T}_w - \overline{T}_{w,wet})] \tag{20}$$

the overprediction is largely eliminated and the standard deviation is significantly reduced (Table 1). The revised correlation now shows less scatter than the original empirical correlation. The relatively high value of $\sigma(R)$ remaining may largely be attributed to the stochastic nature of transition boiling heat transfer.

CONCLUSION

The present study strongly supports the proposition that at high volume fractions in flowing systems, transition boiling wall tem-

perature fluctuations are caused by vertical oscillation of the quench front. This idea is supported both by the visual observations of the present authors and by the temperature measurements made at Argonne National Lab (France et al., 1982). These latter measurements, which show a high cross-correlation coefficient between temperature oscillations at the same axial elevation, can be explained by a vertically oscillating quench front but they are not compatible with the wandering rivulet model previously used. Additional support is provided by the numerical simulation of the wall temperature oscillations which would be produced by a vertically oscillating quench front. The simple model used leads to oscillation magnitudes of the right range and further refinement may be expected to produce improved agreement.

For many of the measurements, the wall temperature oscillations were of sufficient magnitude and clarity so that they could be used for estimating the fraction of time the surface was wetted. By use of results of the numerical model, those wetted area estimates could be correlated with a parameter designated as ΔT_{eff}. It was possible to develop a reasonable prediction of the observed heat transfer coefficients with this wetted area correlation.

It should be pointed out that the present model applies only to transition boiling at high void fractions. The model obviously applies only to the conditions of annular flow where there is a thin liquid layer on the surface of the heater. It should also be noted that if the vertical oscillation of the edge of this liquid film is hydrodynamically controlled, the temperature variation produced may be expected to vary with the heating element used. The relationship between wetted fraction, f, and ΔT_{eff} found to apply in the present situation may not apply to all other systems. It may therefore not be possible to develop a universally applicable heat transfer correlation in terms of only the usual parameters of heat flux, wall and saturation temperatures, vapor fraction, and flow rate. Further, the steady-state model may not apply to transient situations.

ACKNOWLEDGMENT

The authors with to acknowledge the financial support of the Electric Power Research Institute for the experimental program from which the data were obtained. The authors also wish to acknowledge the assistance of James Koren who digitized and performed the Fourier analysis of the temperature oscillation data. In addition, the authors wish to thank Jane-Jane Wang for programming the numerical model and performing most of the numerical calculations.

NOTATION

D = diameter, m
f = wetted fraction
G = mass velocity, kg/m^2·s
k = thermal conductivity, W/m·°C
Pr = Prandtl number
q'' = heat flux, W/m^2
h_b = boiling heat transfer coefficient, W/m^2·°C
h_c = contact heat transfer coefficient, W/m^2·°C
h_{conv} = convective heat transfer coefficient, W/m^2·°C
L = length of the test section, m
r = radial position, m
R = predicted value/measured value
t = time, s
T = temperature, °C
$\overline{T}$ = mean temperature
u_z = mercury velocity, m/s
x = quality (dimensionless)
z = axial position, m

Greek Letters

α = thermal diffusivity, m^2/s
ρ = density, kg/m^3
τ = dimensionless temperature, $(T - T_{\text{sat}})/(T_{m,\text{in}} - T_{\text{sat}})$
μ = viscosity of vapor, kg/s·m
$\mu(R)$ = mean value of R
$\sigma(R)$ = standard deviation of R

Subscripts and Superscripts

0 = outer diameter of the center tube
1 = inner diameter of the outer tube
2 = outer diameter of the outer tube
crit = at critical heat flux conditions
s = stainless steel wall
m = mercury
t = total
w = wall surface
sat = saturation
m,in = mercury at the inlet to the test section
wet = wet
B = vapor at bulk conditions
ℓ = liquid
dry = dry

LITERATURE CITED

Bankoff, S. G., and V. S. Mehra, "A Quenching Theory for Transition Boiling," *IEC Fund.*, **1**, 38 (1962).
Baum, A. J. et al., "Transition and Film Boiling Heat Transfer from Vertical Surfaces," ASME Paper 77-HT-82 (1977).
Berenson, P. J., "Experiments on Pool-Boiling Heat Transfer," *Int. J. of Heat Trans.*, **5**, 985 (1962).
Bjorge, R., G. R. Hall, and N. M. Rohsenow, "Correlation of Forced Convection Boiling Heat Transfer Data," *Int. J. Heat & Mass Trans.*, **25**, 753 (1982).
Chen, J. C., "Correlation for Boiling Heat Transfer to Saturated Fluids in Convective Flow," *IEC Proc. Des. Dev.*, **5**, 322 (1966).
Chen, J. C., R. K. Sundaram, and F. T. Ozkaynak, "A Phenomenological Correlation for Post-CHF Heat Transfer," Lehigh Univ. Report TS-774 (1977).
Chu, C. L., J. M. Robert, and A. W. Dalcher, "DNB Oscillatory Temperature and Thermal Responses for Evaluation Tube Based on Rivulet Model," *J. of Heat Trans.*, **100**, 424 (1978).
France, D. M., et al., "Characteristics of Transition Boiling in Sodium-Heated Steam Generator Tubes," *J. Heat Trans.*, **101**, 270 (1979).
France, D. et al., *Int. J. Heat & Mass Tran.*, **25**, 691 (1982).
Griffith, P., C. F. Avedesian, and J. P. Walkush, "Counterflow Critical Heat Flux," *Heat Transfer Research & Application*, J. Chen, Ed., AICHE Symp. Ser., **74**, 174, 149 (1978).
Hewitt, G. F. et al., "Burnout and Nucleation in Climbing Film Flow," UKAEC Report R4374 (1963).
Kao, Y. K., and J. Weisman, "An Analysis of Wall Temperature Fluctuations in Transition Boiling Heat Transfer," *Basic Mechanism in Two-Phase Flow and Heat Transfer*, R. T. Lahey, Ed., ASME, New York (1980).
Kao, T. T., S. M. Cho, and D. H. Pai, "Thermal Modeling of Steam Generator Tubing under CHF Induced Temperature Oscillations," *Int. J. Heat & Mass Trans.*, **25**, 181 (1982).
McAdams, W. H. et al., *Trans. Inst. Chem. Eng.*, **41**, 1,945 (1949).
Nakanishi, S., et al., "Dryout Phenomena in Shear Flow," *Heat Transfer in Nuclear Reactor Safety*, S. G. Bankoff and N. H. Afgan, Eds., Hemisphere Pub. Corp., Washington, D.C. (1982).
Pei, B. S., "Fundamental Studies of Transition Boiling", M.S. Thesis, Univ. of Cincinnati (1980).
Quinn, E. P., "Forced Flow Heat Transfer to High Pressure Water Beyond the Critical Heat Flux", ASME Paper 63-HT-34 (1963).
Rahgeb, H. S., and S. C. Cheng, "Surface Wetted Area During Transition Boiling in Forced Convective Flow," *J. Heat Trans.*, **101**, 381 (1979).
Villadsen, J., and M. L. Michelsen, *Solution of Differential Equation Models by Polynomial Approximation*, Prentice-Hall, Engelwood Cliffs, NJ (1978).
Wang, S., Y. K. Kao, and J. Weisman, "Studies of Transition Boiling Heat Transfer with Saturated Water at 1-4 Bar," *Nuc. Eng. Des.*, **70**, 223 (1982).
Weisman, J., et al., "Studies of Transition Boiling Heat Transfer with Saturated Water at 1-4 Bar," EPRI Report NP-1899 (June, 1981).

Manuscript received Apr. 11, 1983; revision received Jan. 30, 1984, and accepted Feb. 4.